Journal of Power Sources 197 (2012) 314–318

Contents lists available at SciVerse ScienceDirect

Journal of Power Sources

journal homepage: www.elsevier.com/locate/jpowsour

Short communication

Improving the cyclability of sodium-ion cathodes by selection of electrolyte solvent

C. Vidal-Abarca[a], P. Lavela[a], J.L. Tirado[a,*], A.V. Chadwick[b], M. Alfredsson[b], E. Kelder[c]

[a] Laboratorio de Química Inorgánica, Universidad de Córdoba, Edificio Maire Curie, Planta 1, Campus de Rabanales, 14071 Córdoba, Spain
[b] Functional Materials Group, School of Physical Sciences, University of Kent, Canterbury, Kent CT2 7NR, UK
[c] NanoStructured Materials, Department of Chemical Engineering, TUDelft, 2628BL Delft, The Netherlands

ARTICLE INFO

Article history:
Received 23 July 2011
Received in revised form 31 August 2011
Accepted 4 September 2011
Available online 17 September 2011

Keywords:
Sodium-ion batteries
Sodium iron fluorophosphate
X-ray absorption spectroscopy

ABSTRACT

A composite material containing orthorhombic $Na_{1.8}FePO_4F$ and carbon is prepared by mechanical activation and ceramic procedures. The material is studied in sodium test cells as a potential candidate for sodium-ion battery cathodes. The effect of the solvents in the electrolyte on the electrochemical performance is analysed by X-ray absorption spectroscopy. The structural changes on cycling are small, while the changes in the oxidation state of iron agree with the sodium insertion–extraction processes. The oxidation state is especially affected by the upper limit of the voltage window, and the discharge capacity is strongly affected when using propylene carbonate solvent. Capacity and capacity retention are higher for sodium cells using mixtures of ethylene carbonate and diethyl carbonate as the solvent of $NaPF_6$ electrolytes.

1. Introduction

Sodium-ion batteries have been envisaged as a promising alternative to lithium-ion cells as the current cost and accessibility of lithium may prevent the extensive use of lithium-based batteries. However, sodium electrodes have shown poor cycling properties and this would limit their applications. Almost two decades ago the concept of sodium-ion batteries as an alternative to lithium-ion batteries was discussed by Doeff et al. [1]. In this respect $NaCoO_2$ – the analogue of $LiCoO_2$ – was thoroughly studied as the positive electrode in sodium-ion cells using carbon [2,3] and conversion oxide materials [4] as anodes. Recently, Ellis et al. [5] reported on a sodium/lithium iron phosphate, A_2FePO_4F (A = Na, Li), that could serve as a cathode in either lithium-ion or sodium-ion cells. The use of ionic liquids by Tarascon group has given interesting results on the ionothermal preparation of the sodium fluorophosphates, Na_2FePO_4F, cathode [6].

The optimization of Na_2FePO_4F material for use in sodium test cells is the aim of this work. The study is focused in the changes affecting the cathode material with a common anode on changing the electrolyte. It is well known that safety problems led to discard the use of $LiClO_4$ in lithium-ion batteries. In this study, $NaPF_6$ was chosen instead of $NaClO_4$ in order to avoid safety problems associated to the use of perchlorates. The different organic solvents used in the study are common in lithium and sodium batteries. Firstly, we present a new preparation route based on mechanical activation and ceramic procedures. Then the effect of the electrolyte was analysed by X-ray absorption spectroscopy (XAS). The XAS study of the electrodes was done with different organic solvents. Finally, the choice of electrolyte and potential window were assessed by the analysis of electrochemical results.

2. Experimental

The synthesis of Na_2FePO_4F was carried out in two steps. Firstly, a nano-$FePO_4$ precursor was synthesized by spontaneous precipitation from aqueous solutions as described by Huang et al. [7]. In a second step, the resultant $FePO_4$ was mixed with sodium carboxymethylcellulose (NaCMC, average Mw ~250,000) and NaF (99% purity) in equimolar concentrations and with 10 ml of hot ethanol near the boiling point. The mixture was ground in a planetary ball-mill for 30 min at 500 rpm in air to get a solid–liquid rheological body, a kind of slurry. Finally, Fe^{3+} in the precursor compound ($FePO_4$) was reduced by calcination at 600 °C for 8 h under argon atmosphere.

X-ray diffraction (XRD) patterns were recorded with a Siemens D-5000 apparatus provided with Cu K_α radiation and graphite monochromator. The 2θ scan rate was 0.04° per 1.2 s. Scanning electron microscopy (SEM) was performed in a JEOL-SM6300 microscope.

The electrochemical activity of Na_2FePO_4F/C powder toward Na was measured using Swagelok-type half cells. The test cells

* Corresponding author. Tel.: +34 957218637; fax: +34 957218621.
E-mail address: iq1ticoj@uco.es (J.L. Tirado).

0378-7753/$ – see front matter © 2011 Elsevier B.V. All rights reserved.
doi:10.1016/j.jpowsour.2011.09.008

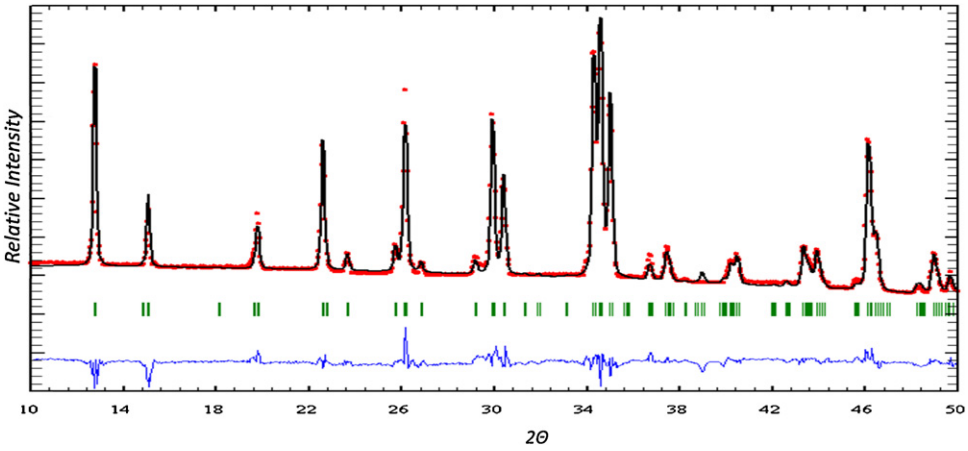

Fig. 1. XRD full-pattern fitting of the as-prepared Na_2FePO_4F/C composite.

were assembled by stacking a sodium metal disk as the negative electrode, Whatman glass fiber disks supporting a 1 M $NaPF_6$ (EC:DEC) (1:1, w/w) or 1 M $NaPF_6$ (PC) electrolytes solution, and the Na_2FePO_4F/C as the positive electrode. The latter was prepared by pasting the electrode material onto an aluminium foil. For this purpose, a mixture of 75% of active material, 15% of carbon black, and 10% of PVDF binder was ball milled for 30 min at 500 rpm in N-methylpyrrolidone (NMP) to form the paste. A VMP-3 multichannel system was used to cycle the cells at C/20 for the cycling between 4.2 and 1.5 V vs Na^+/Na.

^{57}Fe Mössbauer spectra were recorded in transmission mode (TMS) at room temperature, using an EG&G constant acceleration spectrometer and a ^{57}Co (Rh matrix) (10 mCi) γ radiation. The velocity scale was calibrated from the magnetic sextet of a high-purity iron foil absorber. Experimental data were fitted to Lorentzian lines by using a least-squares-based method. The quality of the fit was controlled by the classical χ^2 test. All isomer shifts are given relative to the centre of the α-Fe spectrum at room temperature.

The X-ray absorption studies were performed on BM26 of the DUBBLE – Dutch-Belgian Beam Line – at the ESRF in Grenoble (France). The main characteristics of the beam line are: incident energy range from 4.9 to 32 keV, flux of 1×1011 photons/s, energy resolution dE/E of 2×10^{-4}, horizontal acceptance 2 mrad, beam size at sample place ($H \times V$) max: 30 mm × 3 mm, min: 0 mm × 0.2 mm, and step-by-step data collection with the acquisition time of 1 s for optimised sample. A 9-element monolithic Ge detector with a max. count rate per element ~150 kHz and an energy resolution <250 eV at 5.9 keV for fluorescence measurements at low concentrations was used. An Fe foil was used to calibrate the energy at the edge (7112 eV). The analysis of the absorption data was performed using Sixpack software [8].

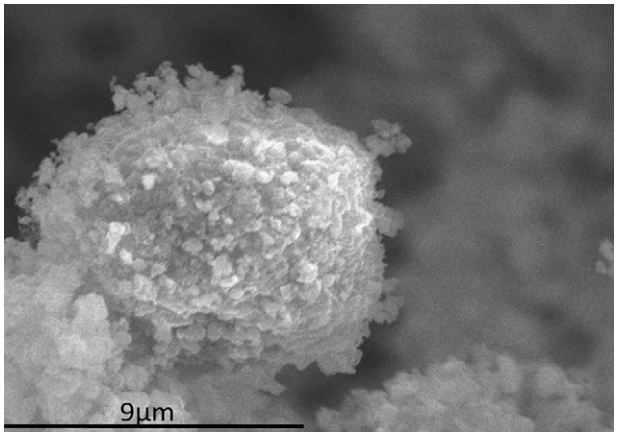

Fig. 2. SEM image of Na_2FePO_4F/C synthesized by solid-state reaction with hot ethanol.

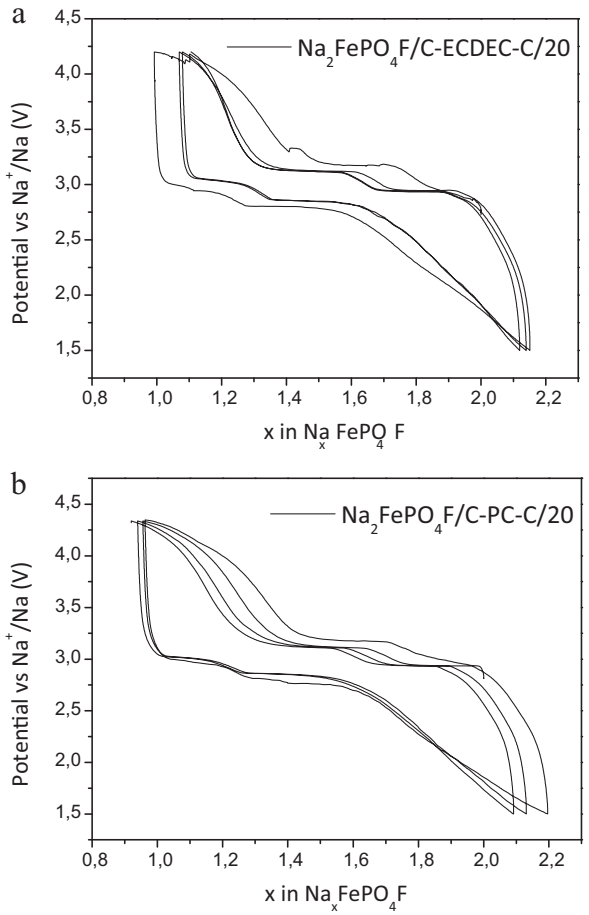

Fig. 3. Charge/discharge galvanostatic curves at C/20 ($1Na^+$ in 20 h) for Na/Na_2FePO_4F/C cells using (a) EC:DEC electrolyte cycled between 1.5 and 4.2 V and (b) PC electrolyte cycled between 1.5 V and 4.3 V vs Na^+/Na.

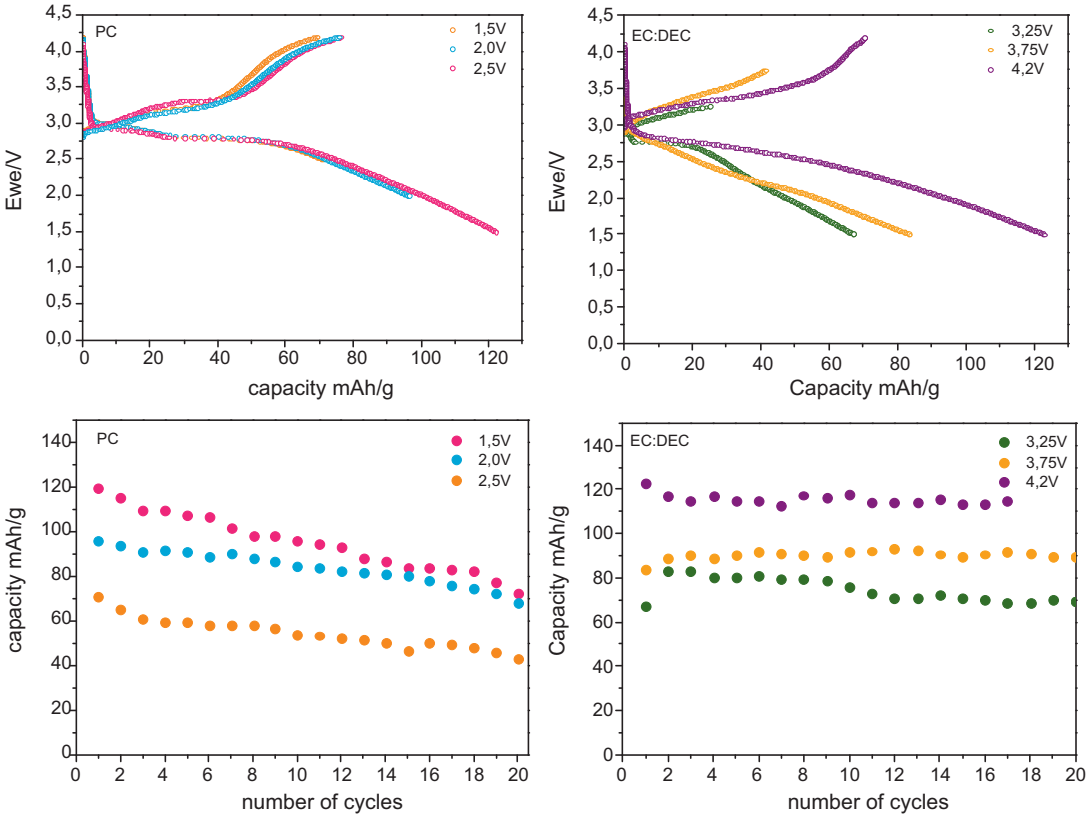

Fig. 4. Upper: charge/discharge galvanostatic profiles using PC electrolyte (left) and EC:DEC electrolyte (right) at different cut-off voltages. Lower: capacity retention data for cycling at C/20 using PC electrolyte (left) and EC:DEC electrolyte (right) at different cut-off voltages.

3. Results and discussion

The X-ray diffraction (XRD) pattern of the resulting Na_2FePO_4F/C composite and the corresponding Rietveld refinement (Fig. 1) confirmed that the phosphate material can be indexed in the orthorhombic *Pbcn* space group in good agreement with previously reported data on Na_2FePO_4F [5]. However, by allowing the refinement of the Na site occupancy, a final stoichiometry of $Na_{1.8}FePO_4F$ with $a = 5.2287_3$ Å, $b = 13.864_1$ Å, and $c = 11.7615_8$ Å. ($R_{wp} = 14.9\%$, $R_{exp} = 14.9\%$, $R_{Bragg} = 8.6\%$) was obtained. The origin of the lower sodium content as referred to stoichiometric Na_2FePO_4F will be further discussed below in the light of the spectroscopic results.

Thermogravimetric analysis was carried out in order to estimate the *in situ* carbon content. The TG curves (not shown) indicated one sharp mass-loss peak between 350 and 450 °C which corresponds to that of carbon removal ($m/m = 25.00$ wt.%). This weigh loss process is related to an exothermic peak in the DTA curve at *ca.* 420 °C due to the release of carbon as volatile oxides. The SEM images showed agglomerates of submicron primary particles (Fig. 2). The presence of Fe^{2+} was confirmed by ^{57}Fe Mössbauer spectroscopy.

Samples were galvanostatically cycled in Na/1 M $NaPF_6$(PC)/Na_2FePO_4F/C and Na/1 M $NaPF_6$ (EC:DEC = 1:1)/Na_2FePO_4F/C cells at C/20. As we can see in Fig. 3, Na/Na_2FePO_4F/C cells reversibly donate *ca.* one sodium at an average voltage of 3 V when cycling at C/20. Good electrochemical results were recorded, featuring capacity values between 100 and 120 mAh g^{-1}. However, depending on the solvents electrolyte decomposition can be observed at end voltages. Using PC, the instability was observed at lower-end voltages while for EC:DEC at the higher-end values of the potential. The charge and discharge profiles and capacity fading were strongly dependent on the used electrolyte.

The electrochemical behaviour is presented in Fig. 4. As PC electrolyte showed instability at lower-end voltages, the upper limit was fixed at 4.2 V, while for lower potentials three different values were used (2.5 V, 2.0 V and 1.5 V). In contrast, the EC:DEC electrolyte showed instability at higher voltages so the lower potential was fixed at 1.5 V and three upper potentials were used (3.25 V, 3.75 V and 4.2 V), as shown in Fig. 4, upper. For both electrolytes a decrease in capacity can be observed when decreasing the voltage window. However, the cell stability depends on the electrolyte, and capacity decreases due to electrolyte decomposition at the end voltages. This is more pronounced for PC. The results revealed

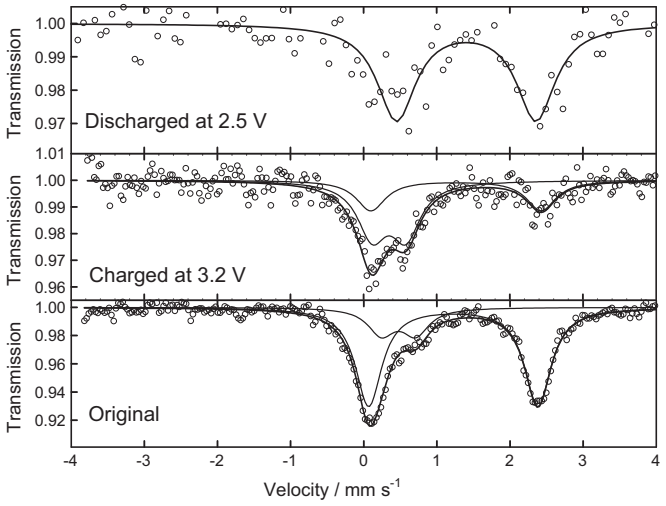

Fig. 5. ^{57}Fe Mössbauer spectra of original and used electrodes at different voltages.

Table 1
Hyperfine parameters of fitted Mössbauer spectra of Na_2FePO_4F/C composite cycled electrodes.

	s/d	Iron species	δ (mm s^{-1})	Δ (mm s^{-1})	Γ (mm s^{-1})	C (%)	χ^2
Original	d	Fe(III)	0.48(2)	0.47(2)	0.44(5)	20.9	0.517
	d	Fe(II)	1.22(1)	2.31(1)	0.44(1)	79.1	
Charged at 3.2 V	d	Fe(III)	0.35(3)	0.46(6)	0.49(4)	63.6	0.524
	d	Fe(II)	1.26(6)	2.3 (1)	0.4(1)	36.4	
Discharged at 1.5 V	d	Fe(II)	1.40(4)	1.91 (6)	0.64(8)	100	0.512

s/d, singlet (s) or doublet (d); δ, isomer shift; Δ, quadrupole splitting; Γ, line-width at half maximum; C, relative contribution; χ^2, goodness of the fitting.

better capacity retention and higher values of capacity for the sodium cells using EC:DEC as the solvent of the electrolyte. Comparing the cycling performances at the same cell voltage window (4.2–1.5 V), it is evident that sodium cells using EC:DEC as an organic solvent, shows distinctly better electrochemical performance (Fig. 4, lower).

The charge–discharge curves show an additional Na uptake. This can be understood from the Fe valency changes. Thus, the ^{57}Fe Mössbauer spectra shown in Fig. 5 and the corresponding fitting results (Table 1) indicate the presence of traces of Fe^{3+} in the original sample. The presence of Fe^{3+} limits the charge capacity, while allowing a deeper reduction of iron after the first discharge. It is stressed that the intensity of the component peaks of the quadrupolar "doublet" of Fe^{2+} signals are typically the same. Therefore, fitting the curve of the sample discharged at 2.5 V, only Fe^{2+} was found, due to the intensity of the peak at ~2.4 mm s^{-1}. The composition derived by Rietveld analysis is clearly correlated with the relative contributions of Fe^{2+} and Fe^{3+} in the Mössbauer spectra. The composition of the initial sample can be more strictly written as $Na_{1.8}Fe^{3+}{}_{0.2}Fe^{2+}{}_{0.8}PO_4$. The oxidation of Fe^{2+} is not complete on charge to 3.2 V, while the reduction to Fe^{2+} is virtually complete during the first discharge, as revealed by the single quadrupole split signal, reaching compositions closer to Na_2FePO_4. However, the deterioration of the quality of the spectra on cycling impeded the use of this technique for further analysis. XAS was used as a successful alternative.

A XANES study on electrodes at various state of charge was carried out here for the first time. The shift of the spectra to higher energies on charge agrees well with the oxidation of iron atoms from 2+ to 3+ (Fig. 6). The reversibility of the process is clear as the capacity is almost completely recovered compared to the initial compound on discharge. The slight but significant shift toward lower energies, as referred to the original compound, after cell discharge agrees well with the extra capacity revealed by the above Mössbauer and electrochemical studies. Thus further sodium can be inserted with the simultaneous reduction of iron below the oxidation state in the original compound. In order to further understand the influence of the electrolyte on the efficiency of the electrochemical reaction with sodium, the spectra at different cut-off voltages were recorded in cells using both electrolytes. The larger differences of line shift with voltage during charging evidence the important role of the electrolyte solvent stability at higher voltages. This behaviour makes it particularly important to use EC:DEC within a moderately high voltage window, as came out from the electrochemical results.

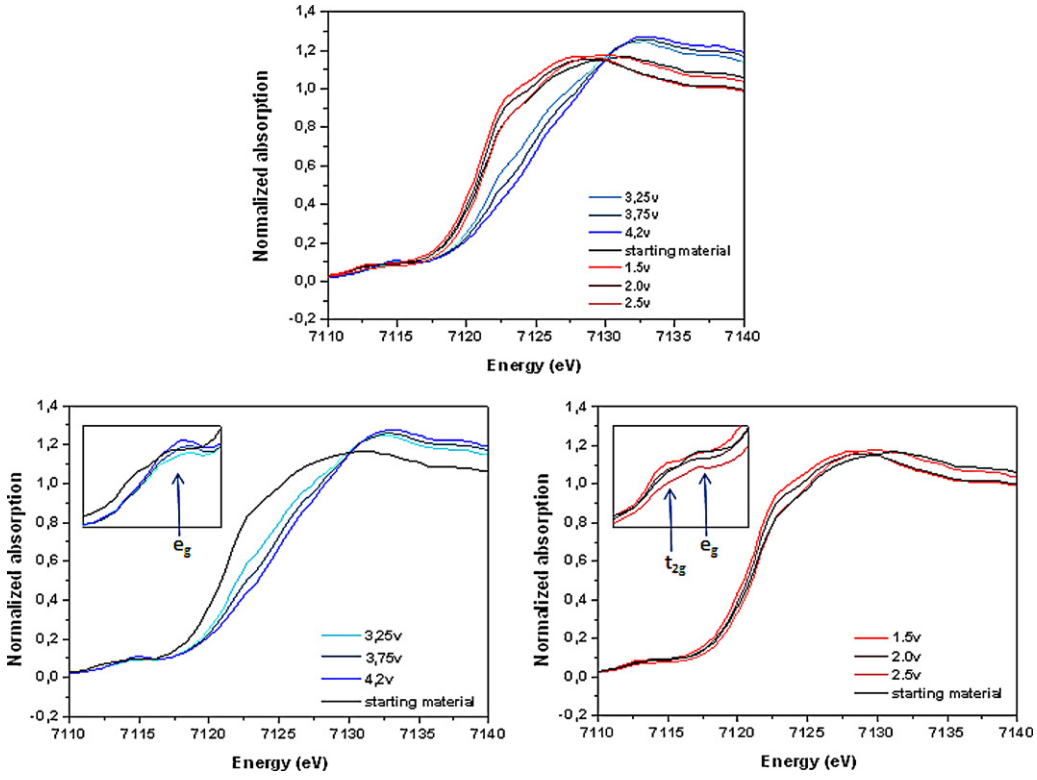

Fig. 6. FeK XANES of Upper: pristine and used electrodes at different voltages. Lower right: details of original sample and charged electrodes. Lower left: details of discharged electrodes.

On the other hand, the intensity of the pre-edge in the spectra of Fig. 6 is indicative of the distortion of the coordination polyhedra, which allows p-d mixing [9]. In fact the cis-FeO_4F_2 units have symmetry lower than Oh. In addition, the t_{2g} and e_g contributions are visible, especially for the original sample, which is indicative of the high-spin configuration of Fe^{2+}. A similar behaviour was reported for the $FePO_4$/$LiFePO_4$ system, in which the Fe K-edge XANES studies revealed that iron in $LiFePO_4$ and $FePO_4$ are both in the expected high-spin state and exhibit a crystal field splitting of about 2 eV [9–11]. For Na_2FePO_4F, the crystal field splitting is slightly larger than 2 eV.

Furthermore, the intensity of the white line increases slightly on oxidation. This behaviour resembles $LiFePO_4$, in which the small changes in intensity were correlated with negligible changes in iron coordination [10–12]. If we assume a change in coordination for Fe that results in a more pronounced p-d mixing, which in turn could decrease the intensity of the white line, this should be accompanied by a sharp increase in the pre-edge intensity, as found in CoC_2O_4 [13]. Moreover, the changes in unit cell parameters from orthorhombic Na_2FePO_4F to $NaFePO_4F$ reported by Ellis et al. [14] and the fact that the structural framework is maintained during cycling according to Trad et al. [15] could imply little distortions. Thus we can conclude that the decreased intensity of the white line is not indicative of abrupt changes in coordination.

4. Conclusions

A new preparation route is found to obtain Na_2FePO_4F/C composites. The resulting material contains the fluorophosphate in the known orthorhombic form, being *ca.* 10% substoichimetric in sodium due to a partial reduction of iron. The composite electrode provides good cycling performance vs sodium in test cells. The local structures of pristine Na_2FePO_4F, and charged and discharged electrodes have been examined by XANES. The results show that Fe^{2+} and Fe^{3+} are found in high spin configurations in discharged and charged electrodes, respectively. The crystal field splitting of Fe^{2+} obtained from the XANES pre-peak is *ca.* 2.3 eV. The structural changes from $Na_{1.8}FePO_4F$ to $NaFePO_4F$, and then to Na_2FePO_4F are small and initiating only slight changes in the intensity of the XANES white line. It is nevertheless stressed, that the choice of the electrolyte is crucial to improve the cycling performance. While the oxidation state is especially affected by the upper limit of the voltage, the discharge capacity is strongly affected when using PC as solvent. The capacity and capacity retention are higher for sodium cells using EC:DEC as solvent using $NaPF_6$ as salt.

Acknowledgements

This work was carried out in the MICINN MAT2008-05880 and Junta de Andalucía FQM-6017 contracts and ALISTORE-ERI.

References

[1] M.M. Doeff, Y. Ma, S.J. Visco, L.C. de Jonghe, J. Electrochem. Soc. 140 (1993) L169.
[2] R. Alcántara, J.M. Jiménez-Mateos, P. Lavela, J.L. Tirado, Electrochem. Commun. 3 (2001) 639.
[3] R. Alcántara, J.M. Jiménez-Mateos, J.L. Tirado, J. Electrochem. Soc. 149 (2002) A201.
[4] R. Alcántara, M. Jaraba, P. Lavela, J.L. Tirado, Chem. Mater. 14 (2002) 2847.
[5] B.L. Ellis, W.R.M. Makahnouk, Y. Makimura, K. Toghill, L.F. Nazar, Nat. Mater. 5 (2007) 749.
[6] N. Recham, J-N. Chotard, L. Dupont, K. Djellab, M. Armand, J.M. Tarascon, J. Electrochem. Soc. 156 (2009) A993.
[7] Y. Huang, H. Ren, Z. Peng, Y. Zhou, Electrochim. Acta 55 (2009) 311.
[8] S.M. Webb, Phys. Scripta 115 (2005) 1011.
[9] H.C. Choi, S.Y. Lee, S.B. Kim, M.G. Kim, M.K. Lee, H.J. Shin, J.S. Lee, J. Phys. Chem. B 106 (2002) 9252.
[10] A. Deb, U. Bergmann, E.J. Cairns, S.P. Cramer, J. Synchrotron Radiat. 11 (2004) 497.
[11] A. Deb, U. Bergmann, E.J. Cairns, S.P. Cramer, J. Phys. Chem. B 108 (2004) 7046.
[12] A. Deb, U. Bergmann, S.P. Cramer, E.J. Cairns, Electrochim. Acta 50 (2005) 5200.
[13] M.J. Aragón, B. León, C. Pérez Vicente, J.L. Tirado, A.V. Chadwick, A. Berko, S.Y. Beh, Chem. Mater. 21 (2009) 1834.
[14] B.L. Ellis, W.R. Michael Makahnouk, W.N. Rowan-Weetaluktuk, D.H. Ryan, L.F. Nazar, Chem. Mater. 22 (2010) 1059.
[15] K. Trad, D. Carlier, L. Croguennec, A. Wattiaux, B. Lajmi, M.B. Amara, C. Delmas, Chem. Mater. 22 (2010) 5554.